External wire coatings: extant and modified

C. Antoinette[1], W. T. Bigbee[2], W. Brostow*[1], G. Granowski[1], H. E. Hagg Lobland[1], N. Hnatchuk[1], R. Pahler[2], A. Richards[1], A. Spagnolo[1], J. Wahrmund[1] and W. Xie[1]

We characterise extant and novel formulations of electrical wire coating materials based on nylons. The materials are for coating commercial grade 600 V copper wire and are evaluated in terms of thermophysical properties, tensile behaviour, static and dynamic friction values and also wear rates from pin on disc tribometry. We study several preparations, i.e. containing various additives, obtained by twin screw mixing followed by pelletising and then compression moulding. Some of our preparations provide lower friction values as well as lower wear rates than the standard commercial nylon compositions.

Keywords: Coatings, Polymer friction, Polymer wear

Introduction

Research on properties of polymeric materials is strongly focused on mechanical properties, achieving high modulus in particular by either processing or reinforcement.[1–3] These while in many instances tribological properties are important. Such is the case of wires for electricity transmission covered with polymeric coatings. Wiring is typically made of copper or aluminium, covered with an internal layer of poly(vinyl chloride) and with an external layer of nylon. The two-layer coating should provide electric insulation, low friction with any contact surfaces, protection from gas and oil and ultraviolet protection. Installation of wiring requires that the wires be pulled through large steel, aluminium or poly(vinyl chloride) conduits or cable trays. Clearly, low friction is important.

While there has been progress in tribology of polymers and polymer based materials,[4–6] much remains to be performed. Encore Wire Corporation, a supplier of electrical wiring, is concerned with the friction and wear resistance of external wire coatings. The issues at stake in considering the performance of such materials have important ramifications for polymer based materials in general and for applications even beyond the specific one of wire coating. In this project, we have prepared and investigated several compositions of external wire coatings, looking for improvement with respect to the standard nylon coating. Thus, we have first determined relevant parameters for commercial nylon (CN) coatings and then begun development of improved formulations of such coatings.

[1]Laboratory of Advanced Polymers & Optimized Materials (LAPOM), Department of Materials Science and Engineering and Department of Physics, University of North Texas, 3940 North Elm Street, Denton, TX 76207, USA
[2]Encore Wire Corp., 1324 Millwood Road, McKinney, TX 75069, USA

*Corresponding author, email wbrostow@yahoo.com

Experimental

Materials

Four CN materials, to be called below CN1, CN2, etc., have been investigated. It is presumed that CN1 is a blend of two nylons. Novel formulations were prepared by mixing CN1 or CN3 with several types of materials. Among these, we have included a polymeric organosilicon compound to be called S1. In addition, we included an engineering thermoplastic that is characterised by high stiffness, low friction and dimensional stability. We have designated this as our low friction polymer (LFP-1) for shorthand purposes. A wear resistant additive (WRA) is also employed; this material is a fluorinated polymer additive. Finally, we have an amorphous high performance thermoplastic included within our range of testing materials; this is to be called N3. Concentrations of these constituents have been varied among the samples.

Sample preparation

Except for 100%LFP-1 and 100%CN1, the materials are melt blended in a Brabender type-six twin screw mixer utilising a 50 g mixing head, effectively supporting a 40 g mixture. In the case of blends, the noted percentages are taken on a weight per cent basis and are prepared at temperatures in the range of 215–255°C (this wide range is due to the variations in the concentrations of constituents) and at a rotation speed of 80 rev min^{-1}. Mixing time ranges from ~5 to 10 min. In the case of the WRA addition to our nylon + LFP-1 blends, a micropipette is used to transfer small amounts of WRA into these blends before mixing in the Brabender.

All of the blends, after being mixed in the Brabender, are pelletised and then compression moulded in a Carver compression moulder. The compression moulder is operated in the temperature range of 235–245°C. Samples are melted for 10 min into 1 mm thick moulding sheets, after which a pressure of 20·7 MPa is

Received 11 January 2013; accepted 30 March 2013
DOI 10.1179/1433075X13Y.0000000109

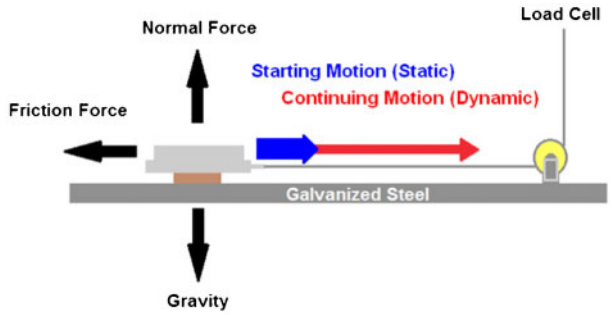

1 Sled testing: 431 g sled is pulled along with sample of interest adhered beneath; static and dynamic friction between surfaces of galvanised steel and sample are measured based on balancing of forces under these respective conditions

applied for 5 min. Samples are cooled to room temperature by flowing water through the compression plates and then stored for characterisation.

Thermogravimetric analysis (TGA)

A Perkin Elmer TGA-7 instrument is used to determine thermal degradation of materials as a function of temperature. Between 5 and 10 mg of each sample is placed into the analyser and heated over the temperature range from 20 to 700°C at a heating rate of 20°C min^{-1}. The instrument measures the weight of the sample as a function of temperature within the specified range. Any changes in weight can then be attributed to mechanisms of thermal degradation, which may be specified through other means. This technique is well described by Menard.[7]

Differential scanning calorimetry (DSC)

Differential scanning calorimetry measurements are performed on both Perkin Elmer DSC-7 and DSC 6000. The instruments measure differences in heat flux between a sample of interest and a reference container, as a function of temperature. This allows location of phase transition temperatures and the values of thermal effects involved. The temperature of the samples is varied from 20 to 250°C, and the heating rate is set to 10°C min^{-1} under N_2 atmosphere at flowrate of 30 mL min^{-1}. A sealed liquid type aluminium capsule pan is used as a sample holder. The sample pan has a volume of 30 μL. Reference pans are developed with the same volume, but without material. This technique is also thoroughly described by Menard.[7]

The melting temperatures T_m, crystallisation temperatures T_c and enthalpies of fusion H^f are evaluated on the basis of the DSC thermograms. The volumetric degree of the crystallinity X_c (%) is calculated as

$$X_c = 100H^f / H^f_{Nylon6} \quad (1)$$

where $H^f_{Nylon6} = 230$ J g^{-1} is the enthalpy of fusion of 100% crystalline Nylon 6.[8]

Tensile and sled testing

An MTS Q-Test 5 mechanical tester is employed to perform tensile testing in accordance with the standard ASTM procedures. The same machine with a friction sled device is implemented to measure static and dynamic friction values. A 10·2 kg (22·5 lb) load cell and a 431 g (0·95 lb) sled are used. The tests are run at the test speed of 150 mm min^{-1} on a galvanised steel surface. The machine measures the resistance to initial and continuous movement across the surface and then quantifies these respectively as the static and dynamic friction for that surface. A schematic of this experiment is shown in Fig. 1.

Pin on disc tribometry and wear determination

Friction tests are conducted on the Nanoevea pin on disc tribometer from Micro Photonics Inc. The tribometer applies a normal load to a sample while moving along a circular path at a selected radius and rotation rate. The measured data provide dynamic friction results. Our tests are performed under the following conditions: temperature of 20°C, rotational speed at 200 rev min^{-1}, wear track radius of 2·0 mm and load that is alternately chosen as 10·0, 15·0 or 20·0 N. The test duration is set to 30 min.

This technique allows also the evaluation of the resulting wear. The wear tracks produced from our pin on disc tribometer are analysed via profilometry. A profilometer calculates the cross-sectional area of the wear track by measuring the profile of the track perpendicular to the track direction. The wear track areas after each pin on disc friction test were determined with a Veeco Dektak 150 profilometer. A stylus with tip radius of 12·5 mm was used. The force applied to the sample was 2·0 mg, and the scan rate was 26·7 mm s^{-1}. The instrument amplifies and records a vertical motion of a stylus displaced at a constant speed by the surface to be measured.[8] A larger area corresponds to more displaced material and therefore higher wear.

Environmental scanning electron microscopy (ESEM) and energy dispersive spectroscopy (EDS)

Energy dispersive X-ray spectroscopy has been used for the elemental analysis of our samples. This was performed using an FEI Quanta ESEM configured with EDS.

This technique measures the emission of X-rays due to the displacement of atomic inner shell electrons. As is well known, the set of discrete energy levels available to atom bound electrons are characteristic of the given atom. Owing to the displacement of inner core electrons, the higher energy electrons fill the available vacancies at lower energy levels, allowing for the emission of a characteristic set of X-rays. The emitted X-ray energies are determined by the differences in electron energy levels. An energy dispersive spectrometer is used to measure the emitted X-rays. This allows determination of the atomic species within a sample.

Thermophysical characterisation

We present TGA results for selected nylon samples in Fig. 1 (left) and the respective derivatives of these curves on the right.

We see in Fig. 2 that CN2 and CN3 samples have similar thermal degradation profiles. Both samples degrade in the 450–550°C temperature range. The amount of thermally degraded material after heating to 700°C is almost the same, equal to 98·9 and 98·8 wt-% for CN2 and CN3 materials respectively.

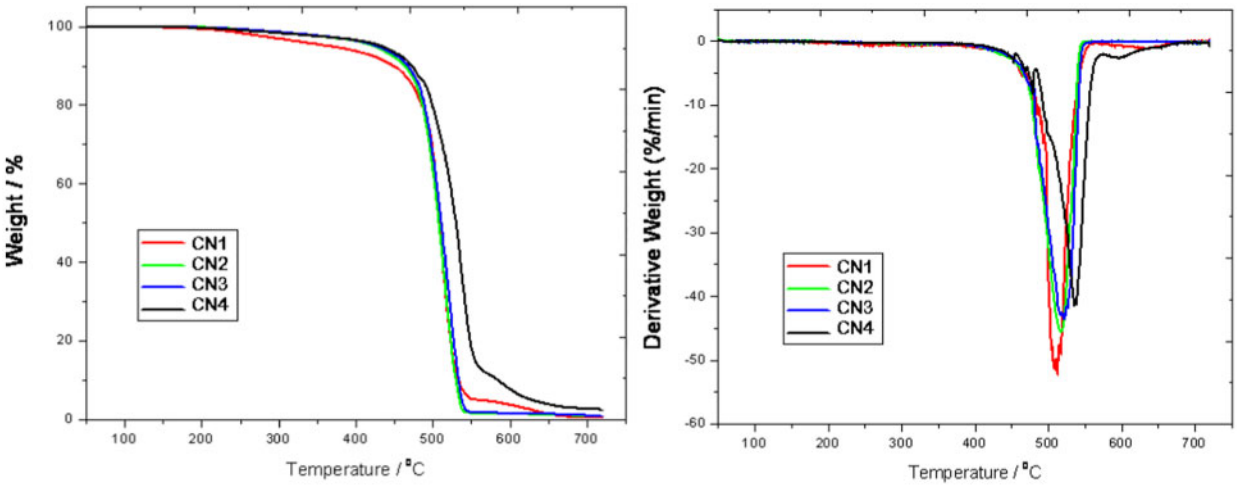

2 Diagrams (TGA) for materials used by Encore Wire Corporation

The weight of CN1 samples decreases slightly starting at 250°C or so. However, similarly to CN2 and CN3, major thermal decomposition of CN1 starts at 450°C. Thermogram (TGA) of CN1 shows a second 'leg' near 550°C. This 'leg' corresponds to a small amount of modifier or additive. That additive does not have high thermal stability, and it does not survive >650°C. The amount of residual material at 700°C is only 1 wt-%.

CN4 also starts to decompose ~450°C. However, compared to the other CN samples, the temperature range of CN4 decomposition is some 5–10°C wider, and a higher temperature is needed for a complete decomposition. Thermal transitions in CN4 take place at slightly higher temperatures than in the other materials investigated. In other words, CN4 has the highest maximum degradation temperature (the temperature at which the material loses the largest part of its original weight).

From Fig. 2, we find also that, with the exception of CN4, most of the CN samples are completely (~99 wt-%) degraded at 550°C. CN4 contains approximately 10–15 wt-% of a high temperature component that survives at 550°C and undergoes further decomposition until 650°C. CN4 samples have 2·8 wt-% of the residual after TGA testing, reflecting the difference in composition between it and other CNs.

To obtain more information about the higher resistance to degradation of CN4, we have performed EDS in combination with ESEM to analyse residues of CN4 after TGA runs. Figure 3 shows energy dispersive spectrum of 'CN4 ash'.

The EDS spectrum tells us that there are three elements inside the 'CN4 ash', namely, C, O and Si. We used ESEM techniques to observe morphology of the CN4 residue. Figure 4 presents low and high magnification ESEM images.

From the ESEM images, we see agglomerated microsized solid particles inside the CN4 ash. These particles can be assigned to the inorganic part of the CN4 that survived after heating the sample at 700°C. Since EDS has detected strong Si and O peaks inside the ash, apparently ESEM shows us solid SiO_2 remaining inside the same sample.

Melting temperature T_m, crystallisation temperature T_c, heat of fusion ΔH^f and the percentage of crystallinity X_c are obtained from non-isothermal crystallisation DSC experiments. An example of a DSC run is presented in Fig. 5. Notice that, for the particular run shown, the melting peak displays a slight asymmetry or 'shoulder'. This feature signifies that an impurity is introduced with the manufacture of CN1. Not all the nylons in this study displayed this shouldering character, as different producers use a different array of additives in their production. Tabulated numerical values are reported in Table 1; they include LFP-1, one of our additives. The quoted accuracy in T_m, namely $\pm 0{\cdot}1$°C, comes from the equipment software but can be viewed with some doubt. Results in the first and last line have been obtained with PerkinElmer DSC 6000, the remaining ones with a PerkinElmer DSC-7 machine.

According to Table 1, the lowest degrees of the crystallinity are found for CN4 samples. We note that two kinds of CN4 samples are analysed through DSC, namely a pellet sample and a sample after melt blending at 215°C. We find that the crystallinity of CN4 decreases after melt blending. This can be understood as a result of decreased polymer chain mobility due to a decrease in free volume and increased viscosity of the blends caused by a filler.

In Fig. 6, we present TGA results for CN1 and also for pure LFP-1 and S1. We see that S1 has distinctly better thermal stability than CN1 and also than other CNs seen in Fig. 1.

Mechanical characterisation of new materials

As noted in the section on 'Materials', nylons can be mixed with a silicon compound S1. Therefore, we prepared a series of materials based on CN1, a typical and apparently widely used CN, and containing varying amounts of that S1.

Table 1 Differential scanning calorimetry data summary

Sample name	T_c/°C	H_C^f/J g^{-1}	T_m/°C	H_m^f/J g^{-1}	X_c/%
CN1	185·4	−57·8	217·7	56·6	24·6
CN2	175·6	−52·2	219·3	34·9	15·2
CN3	166·3	−59·0	214·3	24·3	10·6
CN4 (pellets)	177·3	−45·0	218·0	22·6	9·8
CN4 (blend)	174·3	−46·0	214·7	17·8	7·7
LFP-1	139·1	−131·2	164·1	131·5	…

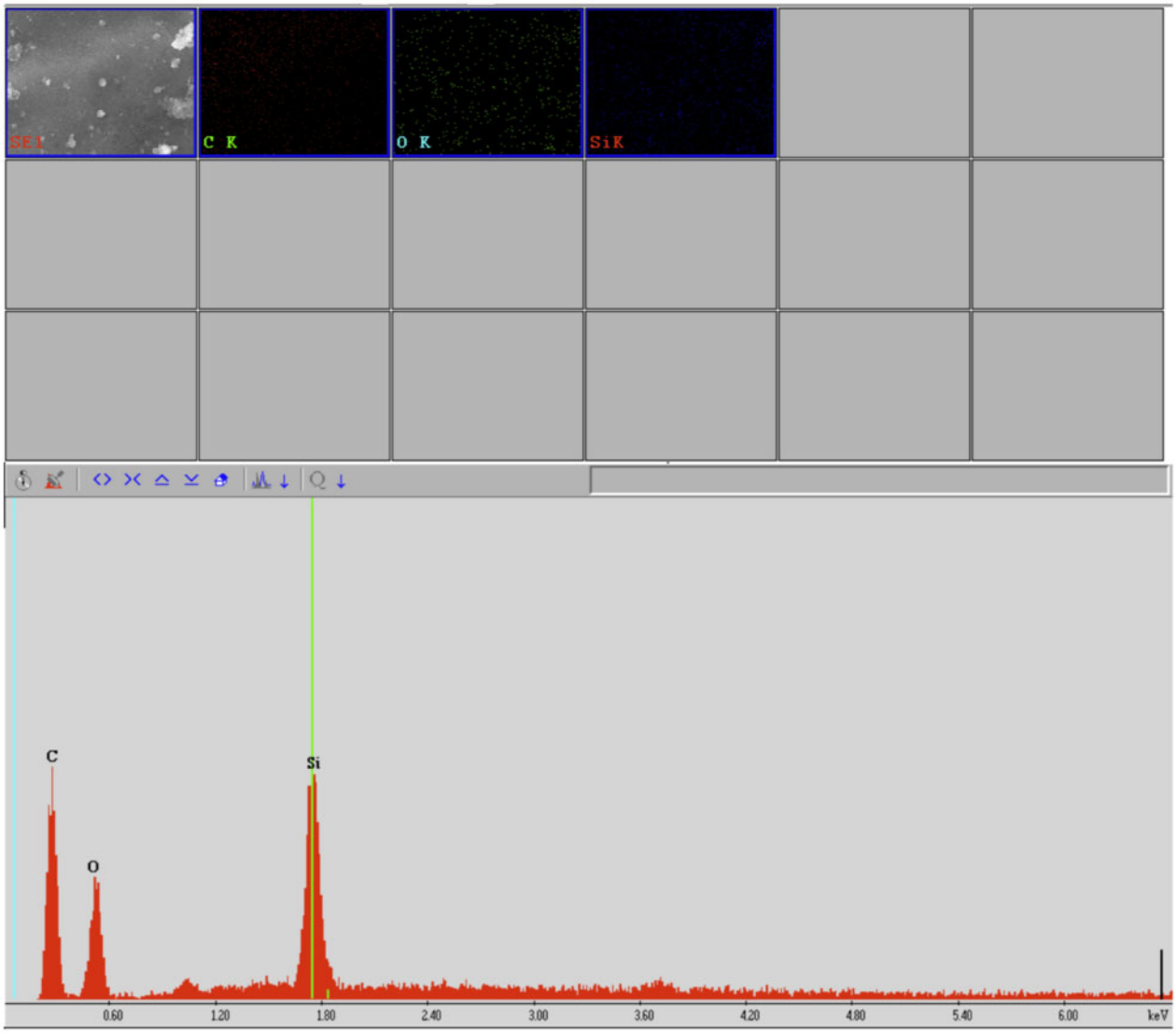

3 Results (EDS) for CN4 ash

Tribological properties of polymers[4–6,9] can be related to mechanical ones.[10] We have performed tensile testing of CN1 + S1 materials. An important property obtained in tensile testing is the strain at break ε_b. It appears in the definition of materials brittleness B,[10,11] namely

$$B = 1/(E'\varepsilon_b) \tag{2}$$

where E' is the storage modulus determined by dynamic mechanical analysis (*see* Ref. 7) at the frequency of

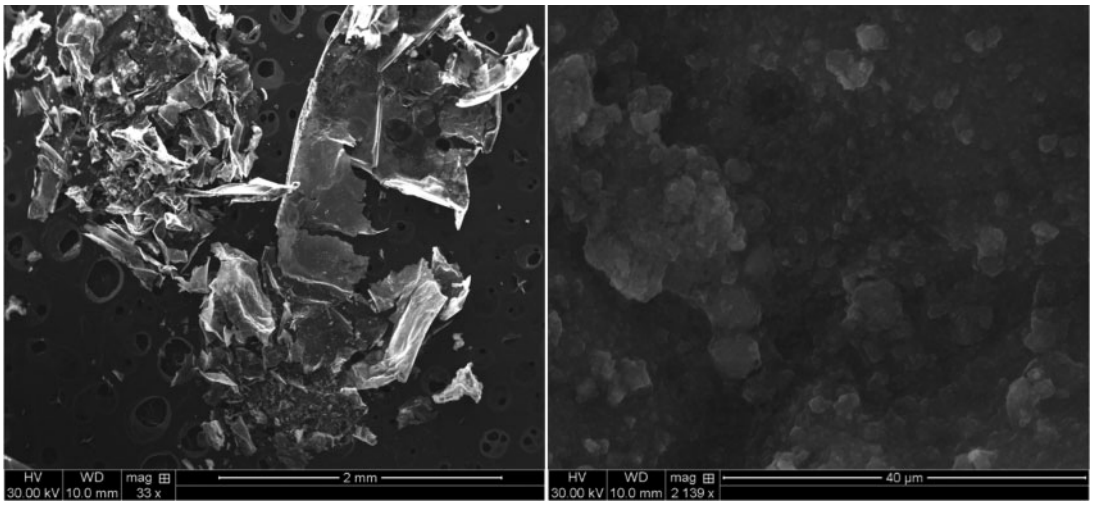

4 Images (ESEM) of CN4 residue after heating at 7000°C

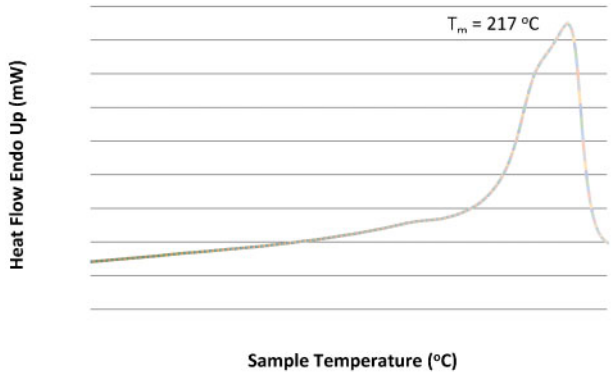

5 Differential scanning calorimetry thermogram for CN (CN1)

1·0 Hz. Results of determination of ε_b as a function of S1 concentration are presented in Fig. 7. Necessarily, we have also determined tensile modulus E as a function of S1 concentration (*see* Fig. 8). In Fig. 8, we have also included a value for a WRA, a material with a clearly higher modulus than the CN1 + S1 blends.

Subsequently, we have developed and investigated a second series of blends based on CN1, but this time with LFP-1 as the additive. We display in Fig. 9 strain at break ε_b values as a function of LFP-1 composition. Tensile modulus E values as a function of the same additive concentration are shown in Fig. 10. In Figs. 7–10, each experimental point is an average of five tests.

As seen in Figs. 9 and 10, acceptable values of the elongation at break along with increased values of the tensile modulus are achieved for the LFP-1 concentration of 10 wt-%. There is an approximate proportionality between the tensile modulus E and the dynamic storage modulus E'.[12] Thus, results in Figs. 7 and 9 and equation (2) suggest that the addition of, say, 10% of LFP-1 to a nylon should lower the brittleness.

Tribological characterisation of new materials

Pin on disc tribometry experiments provide, after an initial period, values of dynamic friction. For all the

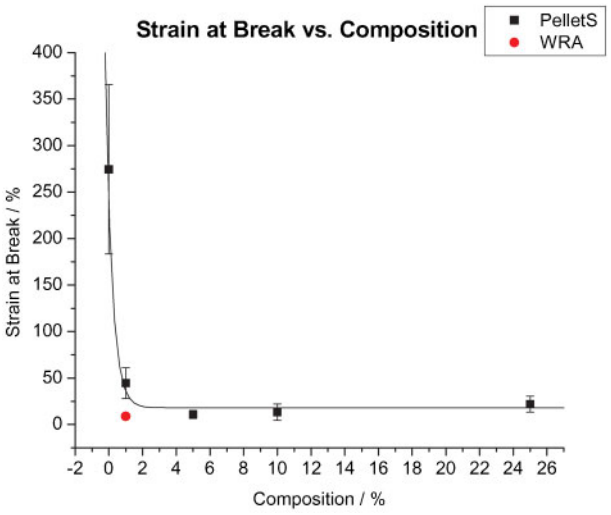

7 Elongation at break as function of S1 concentration in systems based on CN1

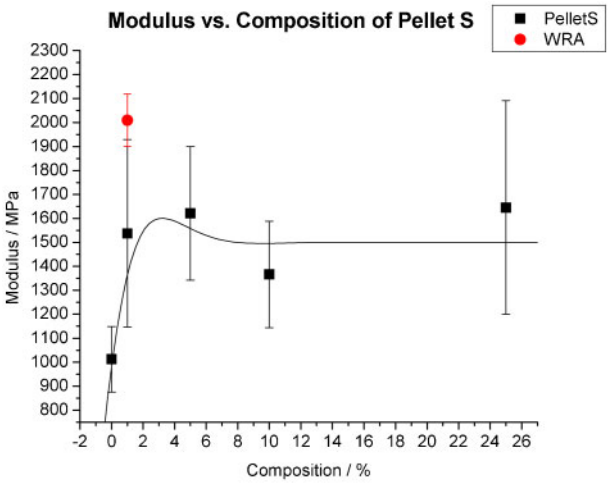

8 Tensile modulus *E* as function of S1 concentration in systems based on CN1

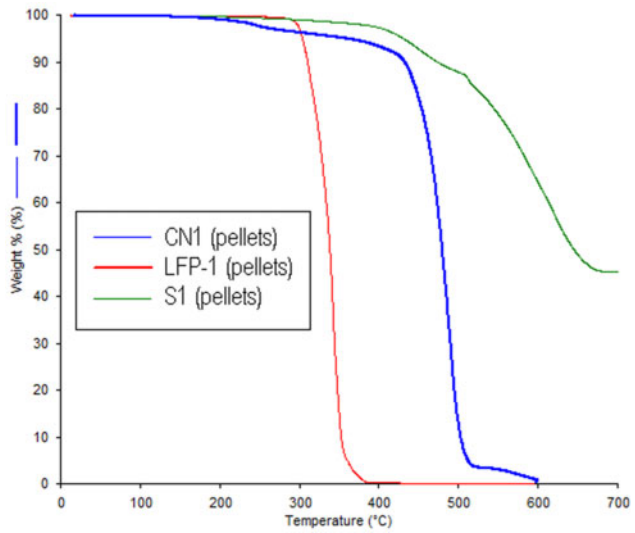

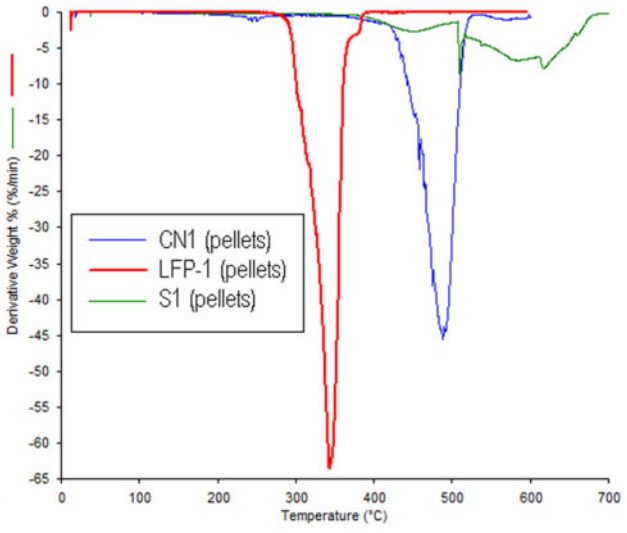

6 Diagrams (TGA) for selected materials (left) and derivative curves (right)

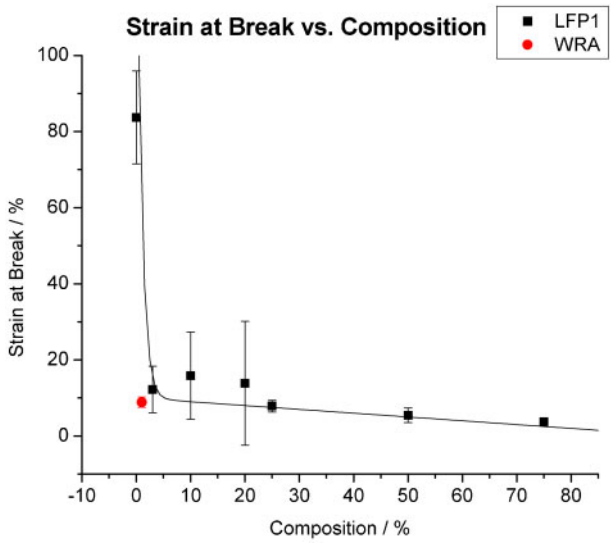

9 Strain at break ε_b values as function of LFP-1 concentration

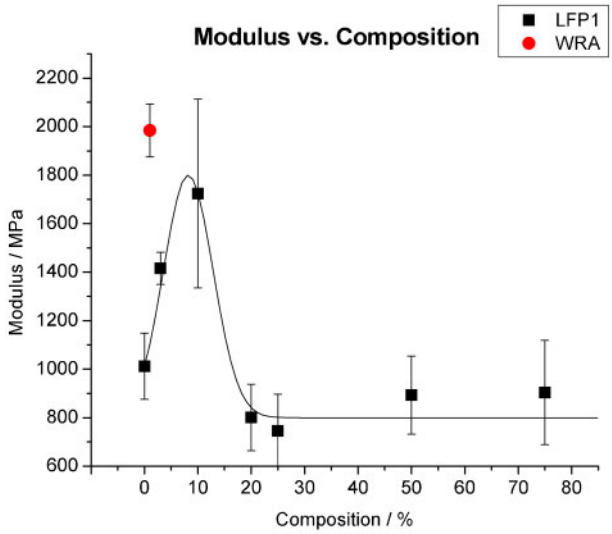

10 Tensile modulus values as function of LFP-1 concentration

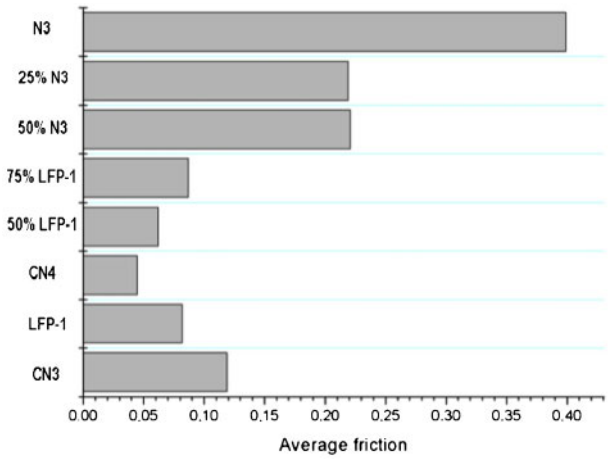

12 Dynamic pin on disc steady state friction values at 10·0 N load: percentages of LFP-1 and N3 in legend correspond to per cent composition in blends with CN3

experiments that follow, the load was selected somewhere in the range between 5 and 20 N (as indicated). These loads are selected on the basis of availability for our apparatus. We anticipate that slightly higher loads would be ideal for simulating the installation process necessary for an industrial setting.

The friction is recorded as a function of distance, as shown, for example, in Fig. 11. The subset of materials reported in Fig. 11 are N3, LFP-1 and CN3 containing, in turn, 25%N3, 50%N3, 50%LFP-1 and 75%LFP-1. Material N3 has the highest dynamic friction of all; however, it is expected to have some processing and other advantages. Note that the friction measurements vary with distance. The steady state values are of greater concern to this study. Steady state values of dynamic friction in Fig. 11 are presented as a block diagram in Fig. 12.

It is evident from Fig. 12 that several materials have lower friction than CN3, while CN4 has the lowest value. Results from a second series of pin on disc testing

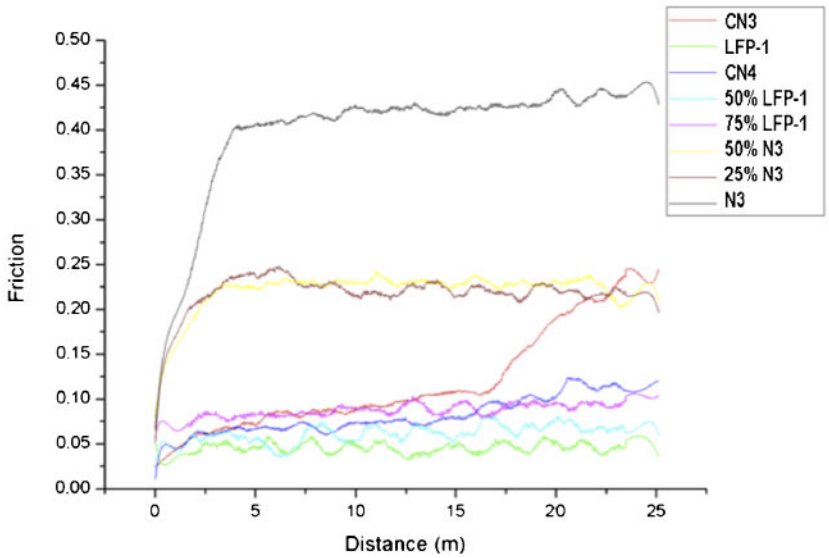

11 Pin on disc dynamic friction at load of 10·0 N as function of distance covered: percentages of LFP-1 and N3 in legend correspond to per cent composition in blends with CN3

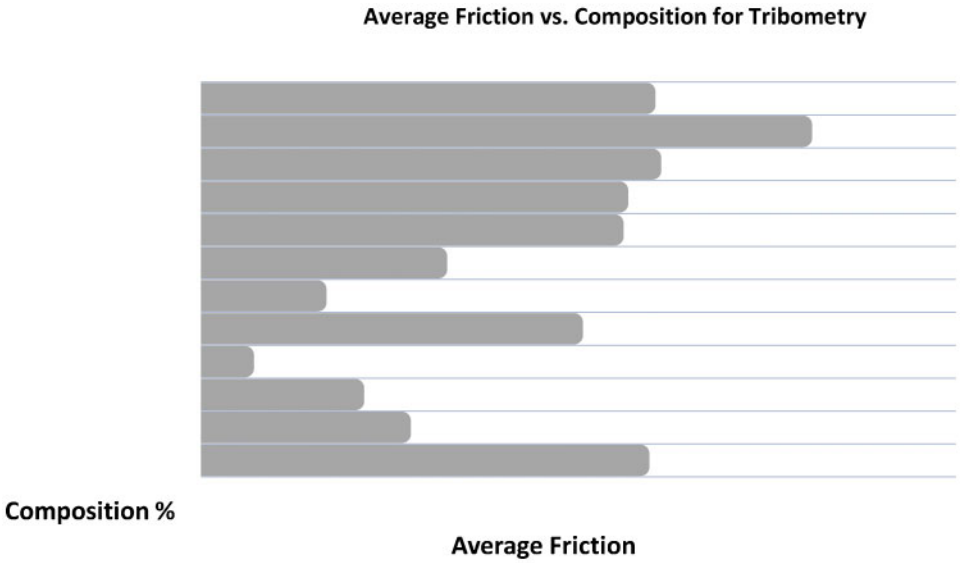

13 Dynamic pin on disc friction values in steady state at 10·0 N for further blends

are presented in Fig. 13. These results represent average friction values under 10·0 N force. The nylon in Fig. 13 is CN1. We see in Fig. 13 that 20 wt-%CN1 + 80%LFP-1 has the lowest friction value among all materials presented in Figs. 12 and 13. Below, we shall discuss also static and dynamic friction values from sled testing.

A set of results from our profilometry measurements is shown in Fig. 14 for the same set of materials presented in Fig. 13. The areas measured by profilometry were gathered from tribometry runs of samples under applied loads of 10, 15 and 20 N. On the basis of these measurements and experimental parameters, we have calculated the wear rate associated with each track created during tribometry testing. The wear rate W for each track is calculated as

$$W = 2\pi rA/(Fd) \tag{3}$$

where r is the track radius, A is the cross-sectional area, F is the load and d is the total distance covered in the tribometry test. The numerator on the right hand side represents the total volume displaced by the tribometer pin during the test. Some results are shown in Fig. 13.

We see in Fig. 14 that the wear rates vary with composition such that the higher concentrations of CN1 produce greater wear on average, particularly in the range of 50–75%CN1. Even the pure CN1 sample under the load of 20 N does not compare well against our blends with LFP-1 under similar loading conditions; LFP-1, while originally aimed at lowering friction, clearly shows also advantageous high wear resistance. The wear rate is reduced by our LFP-1, at the composition 40%CN1 + 60%LFP-1, reflective of similar behaviour observed for the wear track area and for dynamic friction. This finding is important in the development of improved wire coating materials.

As noted in the section on 'Introduction', during installation, coated wires are pulled through large trays, often steel or aluminium. We have, therefore, determined static and dynamic friction values for a number of coatings on steel surfaces. The procedure has been described in the section on 'Tensile and sled testing'. The results are presented in Figs. 15 and 16.

We see in Fig. 16 that CN1 + S1 combinations have higher values of both static and dynamic friction than some other compositions we have developed. Low concentration additives apparently play an important role. For instance, addition of as little as 0·1 wt-%WRA or 0·5 %WRA causes significant lowering of both static

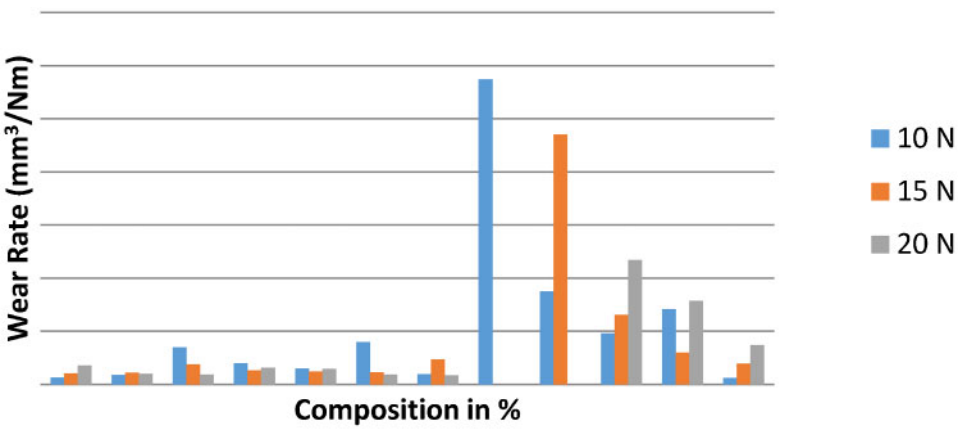

14 Wear rates for samples of varying compositions, tested at several loads

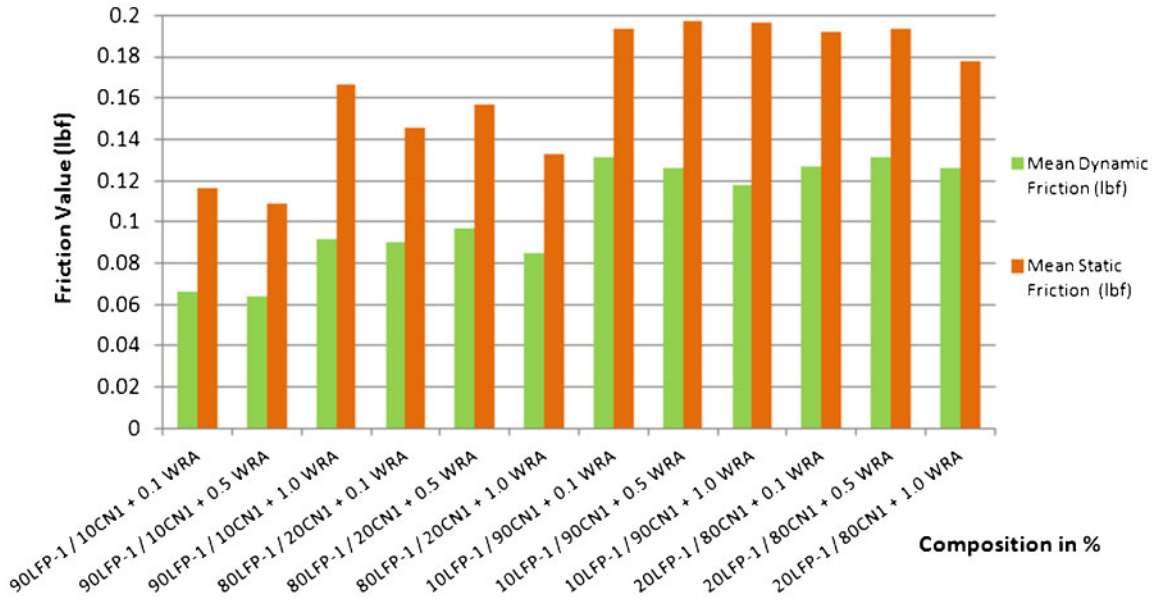

15 Static and dynamic friction values from sled testing

and dynamic friction values as compared with other compositions investigated. We note that sled testing determination of static and dynamic friction typically does not produce wear – while pin on disc tribometry does.

General discussion

Development of improved wire coating materials to be used instead of CNs involves several stages. If a material decomposes at a low T, as determined by TGA, we cannot use it. If a material has a very low T_m, as seen in DSC, it may be too near its molten state and likewise not of use for the present purpose. Materials with high brittleness can be rejected – while tensile testing provides at least partial information on B.

The commercial material CN4 is described by the manufacturer as containing 'organic polymer silicones'. Our EDS results confirm the presence of Si. When dealing with multicomponent systems, we need to take into account miscibility: whether one phase can be formed or whether there arise interfaces in multiphase systems.[13–15]

We saw in Fig. 14 that some of our compositions have clearly higher wear resistance than pure CN1. Lower friction values than pure CN1 have been achieved also, both static and dynamic, as seen in Fig. 16. High tensile modulus can be achieved by additive composition variation, as seen in Figs. 8 and 10. The desired level of obtaining improvements in several properties at the same time is still to be achieved. Ternary, as well as quaternary, systems have to be taken into account in this endeavour. We note that addition of solid fillers is also an option.[16–21]

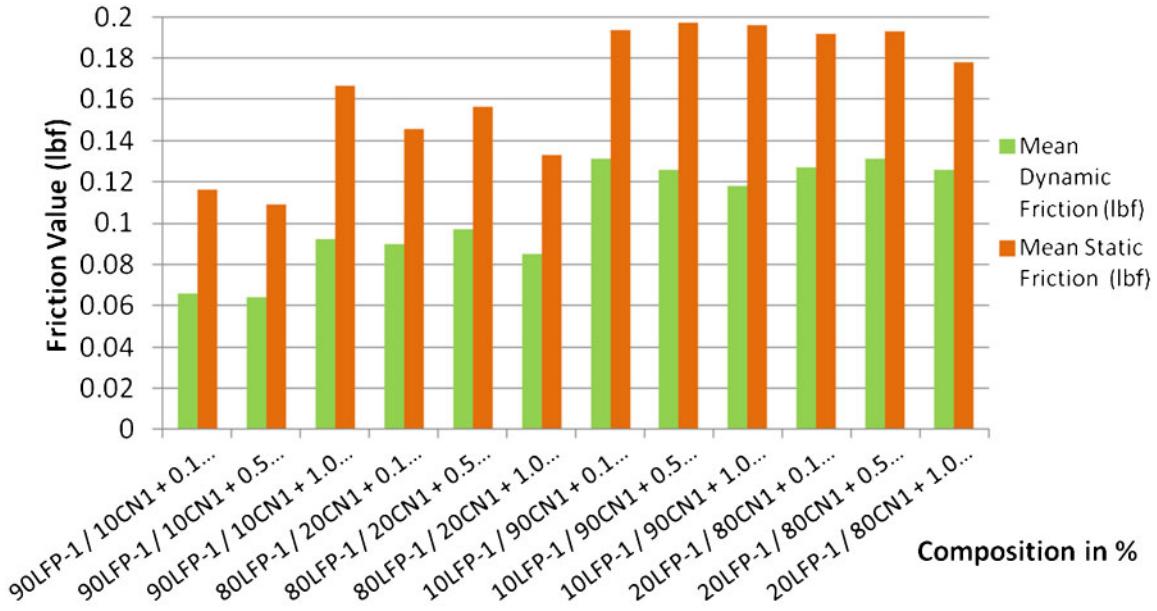

16 Static and dynamic friction values from sled testing continued

Appendix

Formulation	Primary constituent	Secondary constituent	Tertiary constituent
CN1	100% commercial nylon – 1		
CN2	100% commercial nylon – 2		
CN3	100% commercial nylon – 3		
CN4	100% commercial nylon – 4		
LFP-1	100% low friction polymer – 1		
S1	100% Wacker pellet S		
CN1 + WRA	99% commercial nylon – 1	1%WRA	
CN1 + S1	99% commercial nylon – 1	1% Wacker pellet S	
	95% commercial nylon – 1	5% Wacker pellet S	
	90% commercial nylon – 1	10% Wacker pellet S	
	75% commercial nylon – 1	25% Wacker pellet S	
CN1 + LFP-1	97% commercial nylon – 1	3% low friction polymer – 1	
	90% commercial nylon – 1	10% low friction polymer – 1	
	80% commercial nylon – 1	20% low friction polymer – 1	
	75% commercial nylon – 1	25% low friction polymer – 1	
	50% commercial nylon – 1	50% low friction polymer – 1	
	25% commercial nylon – 1	75% low friction polymer – 1	
CN3 + LFP-1	50% commercial nylon – 3	50% low friction polymer – 1	
	25% commercial nylon – 3	75% low friction polymer – 1	
CN3 + N3	50% commercial nylon – 3	50% N3	
	75% commercial nylon – 3	25% N3	
N3	100% N3		
CN1 + LFP-1 (2)	80% commercial nylon – 1	20% low friction polymer – 1	
	75% commercial nylon – 1	25% low friction polymer – 1	
	60% commercial nylon – 1	40% low friction polymer – 1	
	50% commercial nyloncommercial nylon – 1	50% low friction polymer – 1	
	40% commercial nylon – 1	60% low friction polymer – 1	
	30% commercial nylon – 1	70% low friction polymer – 1	
	25% commercial nylon – 1	75% low friction polymer – 1	
	20% commercial nylon – 1	80% low friction polymer – 1	
	15% commercial nylon – 1	85% low friction polymer – 1	
	10% commercial nylon – 1	90% low friction polymer – 1	
LFP-1/CN1 + WRA	10% commercial nylon – 1	90% low friction polymer – 1	+ 0·1% WRA
	10% commercial nylon – 1	90% low friction polymer – 1	+ 0·5% WRA
	10% commercial nylon – 1	90% low friction polymer – 1	+ 1·0% WRA
	20% commercial nylon – 1	80% low friction polymer – 1	+ 0·1% WRA
	20% commercial nylon – 1	80% low friction polymer – 1	+ 0·5% WRA
	20% commercial nylon – 1	80% low friction polymer – 1	+ 1·0% WRA
	90% commercial nylon – 1	10% low friction polymer – 1	+ 0·1% WRA
	90% commercial nylon – 1	10% low friction polymer – 1	+ 0·5% WRA
	90% commercial nylon – 1	10% low friction polymer – 1	+ 1·0% WRA
	80% commercial nylon – 1	20% low friction polymer – 1	+ 0·1% WRA
	80% commercial nylon – 1	20% low friction polymer – 1	+ 0·5% WRA
	80% commercial nylon – 1	20% low friction polymer – 1	+ 1·0% WRA

References

1. L. E. Nielsen and R. F. Landel: 'Mechanical properties of polymers and composites', 2nd edn; 1994, New York, Marcel Dekker.
2. M. S. Rabello: 'Aditivação de polimeros'; 2000, Saõ Paulo, Artliber.
3. E. Pisanova and S. Zhandarov: in 'Performance of plastics', (ed. W. Brostow), Chap. 19; 2000, Munich/Cincinnati, OH, Hanser.
4. W. Brostow, J.-L. Deborde, M. Jaklewicz and P. Olszynski: *J. Mater. Educ.*, 2003, **25**, 119–132.
5. N. K. Myshkin, M. I. Petrokovets and A. V. Kovalev: *Tribol. Int.*, 2005, **38**, 910–921.
6. W. Brostow, V. Kovacevic, D. Vrsaljko and J. Whitworth: *J. Mater. Educ.*, 2010, **32**, 273–290.
7. K. P. Menard: in 'Performance of plastics', (ed. W. Brostow), Chap. 8; 2000, Munich/Cincinnati, OH, Hanser.
8. S. Matsuoka: in 'Handbook of thermal analysis and calorimetry', (ed. S. Z. D. Cheng and P. K. Gallagher), 1st edn, Vol. 3, Chap. 3; 2002, Amsterdam, Elsevier.
9. B. Bhushan: 'Introduction to tribology'; 2002, New York, Wiley.
10. W. Brostow, H. E. Hagg Lobland and M. Narkis: *J. Mater. Res.*, 2006, **21**, 2422.
11. W. Brostow, H. E. Hagg Lobland and M. Narkis: *Polym. Bull.*, 2011, **59**, 1697.
12. Yu. M. Boiko, W. Brostow, A. Y. Goldman and A. C. Ramamurthy: *Polymer*, 1995, **36**, 1383.
13. A. Kopczynska and G. W. Ehrenstein: *J. Mater. Educ.*, 2007, **29**, 325.
14. R. C. Desai and R. Kapral: 'Dynamics of self-organized and self-assembled structures'; 2009, Cambridge, Cambridge University Press.
15. G. H. Michler and F. J. Balta-Calleja: 'Nano- and micromechanics of polymers: structure modification and improvement of properties'; 2012, Munich, Hanser.
16. Z. Roslaniec, G. Broza and K. Schulte: *Compos. Interfaces*, 2003, **10**, 95.
17. R. H. Krämer, M. A. Raza and U. W. Gedde: *Polym. Degrad. Stab.*, 2007, **92**, 1795–1802.
18. A. Pegoretti, A. Dorigato and A. Penati: *Express Polym. Lett.*, 2007, **1**, 123–131.
19. G. Broza and K. Schulte: *Polym. Eng. Sci.*, 2008, **48**, 2033.
20. A. Szymczyk, Z. Roslaniec, M. Zenker, M. C. Garcia-Gutierrez, J. J. Hernandez, D. R. Rueda, A. Nogales and T. A. Ezquerra: *Express Polym. Lett.*, 2011, **5**, 977–995.
21. R. Adhikari, W. Brostow, T. Datashvili, S. Henning, B. Menard, K. P. Menard and G. H. Michler: *Mater. Res. Innov.*, 2012, **16**, 19.